SYNTHESIS AND CHARACTERIZATION OF ZEOLITE LSX FROM RICE HUSK SILICA

Pongtanawat Khemthong, Sanchai Prayoonpokarach and Jatuporn Wittayakun*

Received: Jun 14, 2007; Revised: Aug 14, 2007; Accepted: Aug 16, 2007

Abstract

Silica powder with approximately 98% purity was extracted from rice husk (RH), converted to a sodium silicate solution, and used as a silica source for the synthesis of low silica type X (LSX) by hydrothermal process. The synthesized zeolite in the form of Na and K cations, referred to as NaK-LSX, was characterized by X-ray diffraction (XRD) and Fourier transform infrared spectroscopy (FTIR), which confirmed the success of the synthesis. Images from scanning electron microscopy (SEM) of NaK-LSX displayed multi-faceted spherulite particles composed of polycrystal particles with different sizes along with small amorphous particles. The particle size distribution of NaK-LSX from a laser diffraction particle size analyzer (DPSA) was in the range of 0.2 - 50 μm and nitrogen adsorption indicated a surface area around 400 m^2/g. The structure of LSX did not change after the ion-exchange to produce an ammonium form but collapsed after subsequent calcination.

Keywords: Rice husk silica, NaK-LSX, zeolite, hydrothermal

Introduction

The composition of rice husks varies with geological location. Mainly it contains organic substance and approximately 20% wt of silica (SiO_2) and after combustion the white ash contains approximately over 90% wt of SiO_2 (Kapur, 1985; Hamdan *et al.*, 1997; Williams and Nugranad, 2000; Huang *et al.*, 2001; Park, 2003). There are impurities in rice husk ash such as oxides of alkali metal which could be removed by leaching rice husk with acids before calcination; such a method could improve the purity of rice husk silica (RHS) to 96 - 99 % wt. (Williams and Nugranad, 2000; Sun and Gong, 2001; Chorkendorff *et al.*, 2003; Liou, 2004; Prasetyoko *et al.*, 2005). With high purity, RHS has potential as a silica source for the production of silicon-based inorganic materials such as silicon carbide (SiC); silicon nitride (SiN); mesoporous silica including MCM-41 and MCM-48; and zeolites (Wang

School of Chemistry, Institute of Science, Suranaree University of Technology, Nakhon Ratchasima 30000, Thailand, Tel.: 0-4422-4256; Fax.: 0-4422-4185; E-mail: jatuporn@sut.ac.th

* *Corresponding author*

et al., 1998; Huang *et al.*, 2001; Sun and Gong, 2001; Grisdanurak *et al.*, 2003; Katsuki *et al.*, 2005; Prasetyoko *et al.*, 2006). This study focuses on using RHS as a silica source for the synthesis of low silica zeolite type X (LSX).

Zeolites are microporous crystalline aluminosilicates in which the structural framework contains tetrahedral TO_4 units (T = Si or Al) linked together by oxygen sharing (Corma, 2001). The general formula of zeolite is $M_a^{n+}[Si_xAl_yO_z] \cdot mH_2O$ where M_a^{n+} are extra-framework cations; $[Si_xAl_yO_z]$ is the zeolite framework; and mH_2O are sorbed water molecules (Roberie *et al.*, 2001). Zeolites are related to several industrial applications, for example they are catalysts in fluid cracking, sorbents in volatile organic removal (Cundy *et al.*, 2005), a solid-state hydrogen storage medium (Langmi *et al.*, 2005; Li and Yang, 2006), and an internal side space for synthesis of transition-metal encapsulation (Salavati-Niasari *et al.*, 2006).

Zeolite LSX is in the faujasite (FAU) family with a framework containing double 6 rings linked through sodalite cages that generate supercages with pore diameters of 7.4 Å. The typical Si/Al ratio of LSX is in the range of 1 - 1.5. It belongs to the space group F_{3m} (Auerbach *et al.*, 2003) and has a large number of extra-framework cations. LSX can be synthesized from a variety of silica sources including natural clay such as kaolinite, oil shale ash, and commercial silicates (Chandrasekhar and Pramada, 2001a, 2002b; Machado and Miotto, 2005). There are no reports on the synthesis of LSX with a silica source from rice husk.

Here we report the synthesis of zeolite LSX with the formula $Na_{73}K_{22}[Si_{97}Al_{95}O_{384}] \cdot 212H_2O$ (Esposito *et al.*, 2004) by using RHS as a silica source and characterization by X-ray diffraction (XRD), Fourier transform infrared spectroscopy (FTIR), surface area analysis (BET), scanning electron microscopy (SEM), and laser diffraction particle size analyzer (DPSA). Its stability after ion exchange to ammonium and proton forms (NH_4-LSX and H-LSX, respectively) was studied by thermogravimetric analysis (TGA).

Experimental

Materials for RHS Extraction and Zeolite Synthesis

Hydrochloric acid (37% HCl, Carlo-Erba), sodium silicate solution (Na_2SiO_3; 28.7% SiO_2, 8.9% Na_2O, Panreac, N Brand clarified), sodium aluminate (~55 - 56% of $NaAlO_2$, Riedel-de Haën), sodium hydroxide (97% NaOH, Carlo-Erba), potassium hydroxide (85% KOH; Ajax Fine Chem), ammonium nitrate (99.0% NH_4NO_3, J. T. Baker), and rice husk for RHS (local rice mill in Lampang, Thailand).

Silica Extraction from Rice Husk

Rice husk was washed thoroughly with water to remove the adhering soil and dust and dried at 100°C overnight. The dried rice husk then was refluxed in 3M HCl solution for 6 h, filtered and washed repeatedly with water until the filtrate was neutral and dried in an oven at 100°C overnight. Finally, the refluxed rice husk was pyrolyzed in a hot air furnace muffle (Carbolite, CWF1200) at 550°C for 3 h to remove the organic contents to obtain the white RHS.

Synthesis of Zeolite LSX

The LSX synthesis was synthesized by hydrothermal method with an initial batch composition of 5.5 Na_2O : 1.65 K_2O : Al_2O_3 : 2.2 SiO_2 : 122 H_2O prepared from sodium silicate and sodium aluminate solution with a method modified from that described by Kühl (2001). The sodium silicate solution was prepared by slowly adding RHS into 100 mL of 14% wt NaOH solution under stirring until a homogeneous solution was obtained. In the LSX synthetic procedure, sodium aluminate was dissolved in deionized water and slowly added into a solution containing KOH and NaOH. The new solution was mixed with diluted sodium silicate solution. The resulting mixture was transferred into a polypropylene bottle, capped and sealed with paraffin film. Aging and crystallization were carried out at 70°C for 3 h without stirring, then adjusted to 100°C for 2 h to complete crystallization; the sample was cooled down to room temperature and washed with water and

0.01 N NaOH solution, and dried at 110 - 125°C overnight. The obtained product was zeolite LSX in the form of Na and K cations and was designated as NaK- LSX throughout this article.

Characterization of RHS and NaK- LSX

The chemical compositions of RHS in the form of oxides were analyzed by energy dispersive XRF (EDS Oxford Instrument ED 2000) with an array of 16 anodes analyzing crystals and Rh X-ray tube as a target with a vacuum medium.

Phase and crystallinity of RHS and NaK-LSX were confirmed by powder XRD (Bruker AXS diffractometer D5005) with nickel filter Cu K_α radiation scanning from 4 to 50° at a rate of 0.05 °/s with current 35 kV and 35 mA.

Functional groups within the NaK-LSX structure were identified by FT-IR (Spectrum GX, Perkin-Elmer) using KBr as a medium. IR spectra were scanned in the range of 4,000 cm^{-1} to 400 cm^{-1} with a resolution of 4 cm^{-1}.

The specific surface areas (BET), pore volumes, and pore sizes of NaK-LSX were determined from a nitrogen adsorption isotherm by a Quantachrome (NOVA 1200e) gas adsorption analyzer at liquid nitrogen temperature. The sample was degassed at 300°C for 3 h before the measurement.

Crystallite size and morphology of NaK-LSX were studied by SEM (JEOL JSM-6400) with applied potential 10 - 20 kV.

Particle size distribution of NaK-LSX was determined by DPSA (Malvern Instruments, Mastersizer 2000) with the sample dispersed in distilled water and analyzed by He-Ne laser. The standard volume percentiles at 10, 50, and 90, or denoted as d(0.1), d(0.5), and d(0.9), respectively, were recorded from the analysis and used to calculate the width of the distribution. The width was calculated from the equation below:

$$\frac{d(0.9)-d(0.1)}{d(0.5)}$$

Finally, NaK-LSX was exchanged to NH_4-LSX by stirring in NH_4NO_3 for 18 h. After filtration and drying, the obtained NH_4-LSX product was calcined at 400°C to convert to H-LSX. Thermal stabilities of NH_4-LSX were investigated by TGA on a Simultaneous Differential Thermal Analysis (SDT 2690) by heating from room temperature to 1,000°C with a heating rate of 10°C/min in nitrogen flow (100 ml/min). The phases of both materials were also analyzed by XRD.

Results and Discussion

RHS Characterization

The chemical compositions of RHS in the form of oxides are shown in Table 1. The major component was SiO_2 along with small amounts of Al_2O_3, K_2O, CaO and Fe_2O_3. The purity of RHS was sufficient to use as a silica source for the synthesis of NaK-LSX. The purity from this study was higher than that of rice husk ash (RHA) obtained from combustion without leaching which was less than 95% (Kapur, 1985; Williams and Nugranad, 2000; Huang *et al.*, 2001; Liou, 2004). However, that silica from RHA was still suitable for the synthesis of several porous materials such as MCM-41, zeolite beta, and zeolite ZSM-5 (Sun and Gong, 2001; Prasetyoko *et al.*, 2006).

The powder XRD pattern of RHS is shown in Figure 1. Only a broad peak at approximately 22 degrees which was a characteristic of amorphous silica was observed. This phase was more suitable for the NaK-LSX synthesis than the crystalline form because it could be dissolved to form sodium silicate more easily. A longer time would be needed in the synthesis with crystalline silica (Hamdan *et al.*, 1997).

Characterization of NaK-LSX by XRD

The formation of the NaK-LSX framework synthesized from RHS was confirmed by XRD comparing with standard NaX (Figure 2). The sample gave peaks at positions similar to that of the standard NaX, indicating the formation of the faujasite structure, and the sharp peaks indicated high crystallinity. The relative crystallinitiy to the standard NaX was calculated in the equation below (Gosh *et al.*, 1994; Tangkawanit and Rangsriwatananon, 2004) and the obtained value was approximately 100%:

Table 1. RHS components determined by XRF

Components	(%wt)
SiO_2	97.96
Al_2O_3	00.56
K_2O	00.06
CaO	00.98
Fe_2O_3	00.02

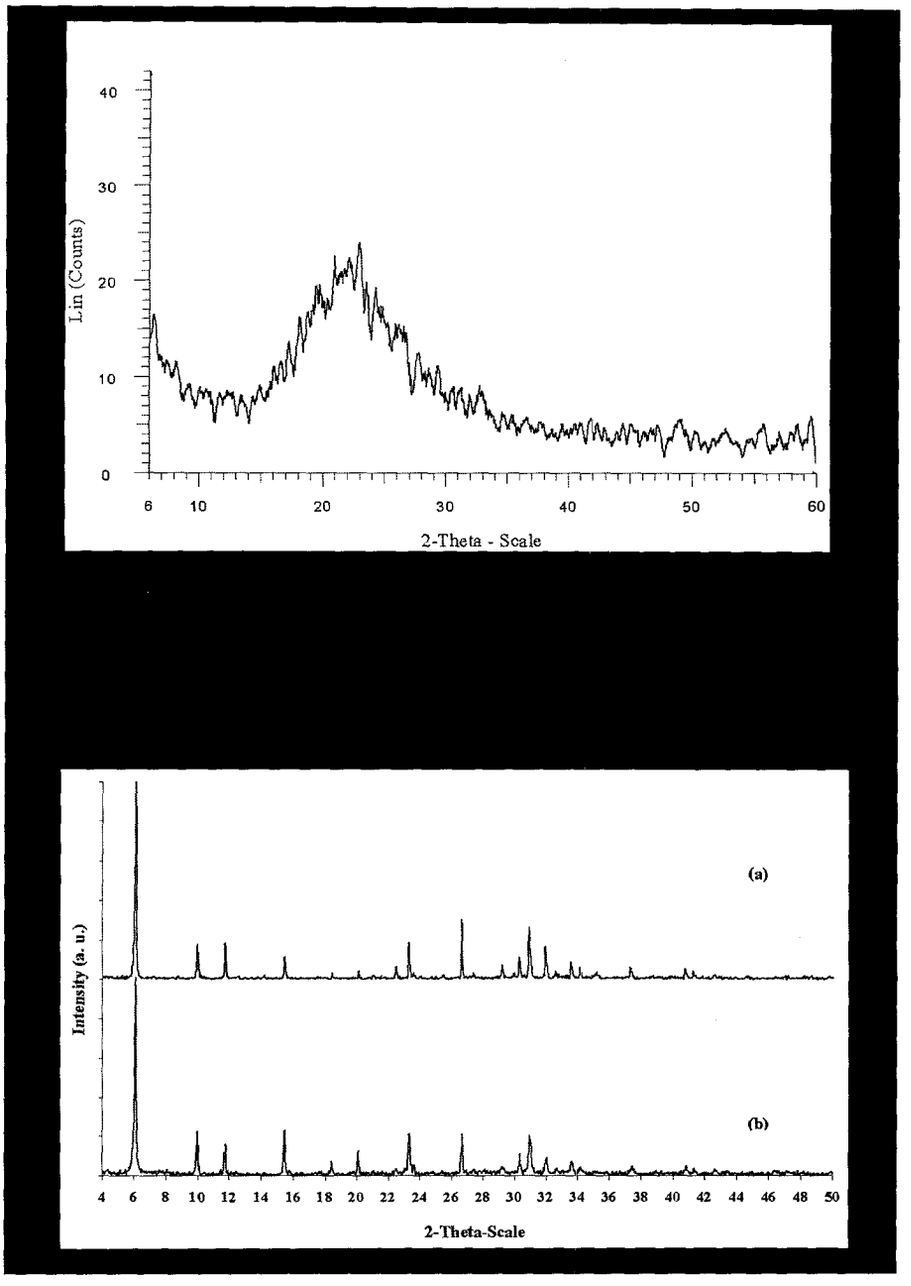

Figure 2. XRD spectrum of (a) NaK-LSX synthesized from RHS and (b) standard NaX

$$\%Crystallinity = \left(\frac{\sum^{i2} intensity\ of\ XRD\ peak\ of\ product}{\sum^{i2} intensity\ of\ XRD\ peak\ of\ standard\ zeolite\ NaX} \right) \times 100$$

The details of peak positions, d-spacing and relative intensity of NaK-LSX and standard NaX are presented in Table 2. Although all the XRD peaks of NaK-LSX were similar to those of the standard NaX, the sequence of intensities were different. This was not surprising because our sample contains both Na and K cations, while the standard only has the Na cation. It was previously reported that the sequence of peak intensities depended strongly on type of cations (Joshi *et al.*, 2002; Esposito *et al.*, 2004) and the presence of K^+ attenuated them. Moreover, the lower Si/Al ratio enhanced the line intensities (Kühl, 1987).

Characterization of NaK-LSX by FTIR

The synthesized NaK-LSX was characterized by FTIR to identify functional groups in the structure. Figure 3 shows a strong peak at 950 cm^{-1} which was assigned to an asymmetric T-O stretching. In general, T-O is a tetrahedral atom referred to the framework of Si, Al composition and may shift to a lower frequency with an increase of the number of tetrahedral Al atoms (Lee *et al.*, 2006). Bands in the region 773 cm^{-1}, 690 cm^{-1} and 571 - 460 cm^{-1} were attributed mainly to the symmetric stretching, double ring and T-O bending vibrations, respectively. Lee *et al.* (2006) and Sang *et al.* (2006) reported that a band at 600 - 500 cm^{-1} is related to the topological arrangement of secondary units of structure in zeolites that contain the double 4 and 6 rings external linkage peak associated with the FAU structure and also observed in all the zeolite structures. The band with a peak at 3,487 cm^{-1} was assigned to OH stretching and the vibration at 1,638 cm^{-1} was referred to bending vibration of adsorbed water molecule (Dyer *et al.*, 2004).

Surface Analysis of NaK-LSX by BET

The N_2 adsorption isotherm of NaK-LSX is shown in Figure 4. It was type I based on IUPAC's classification with a large nitrogen uptake at low pressure and the desorption almost overlapping with the adsorption. The step increased in N_2 adsorption with an increased relative pressure, P/P_0 and N_2 adsorbed amount reaching 127 cm^3/g at $P/P_0 = 0.048$ suggesting the pressure of an appreciable amount of micropore on the NaK-LSX surface. This result was common for the zeolite structure as explained by Langmi *et al.*(2005) that zeolite X has a very open framework and the entries to

Table 2. Peak positions, d-spacing and relative intensity of NaK-LSX and standard NaX

		Relative intensities	
2θ	**d**	**Standard NaX**	**Synthesized LSX**
6.10	14.48	100.00	100.00
15.43	5.74	22.70	13.10
9.99	8.85	22.40	17.30
26.70	3.34	22.10	29.40
23.32	3.81	21.00	20.00
30.10	2.88	20.40	26.20
11.73	7.54	16.40	17.80
20.09	4.42	12.60	6.90
30.36	2.94	11.21	13.10
32.03	2.79	8.62	17.30
18.43	4.81	7.18	4.20
34.24	2.62	4.89	6.20

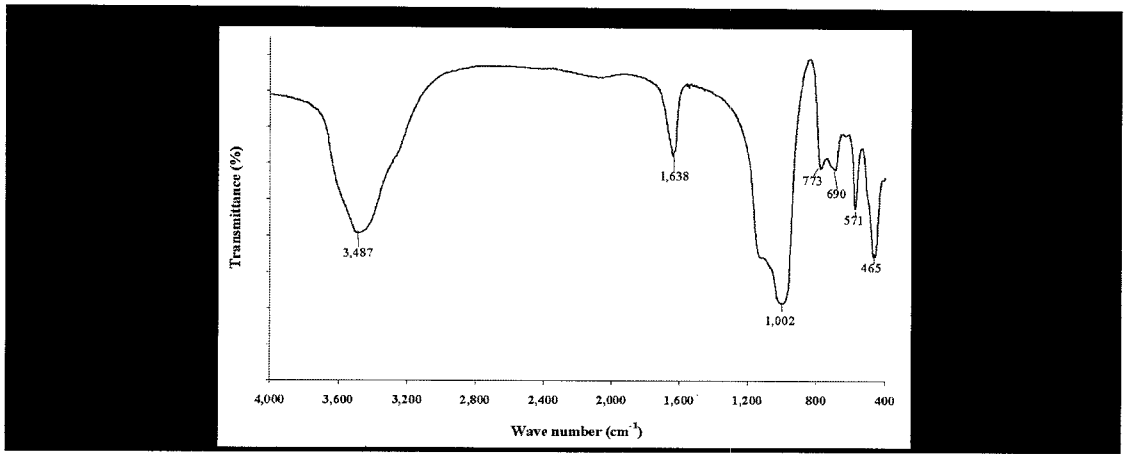

Figure 3. IR spectrum of zeolite NaK-LSX synthesized from RHS

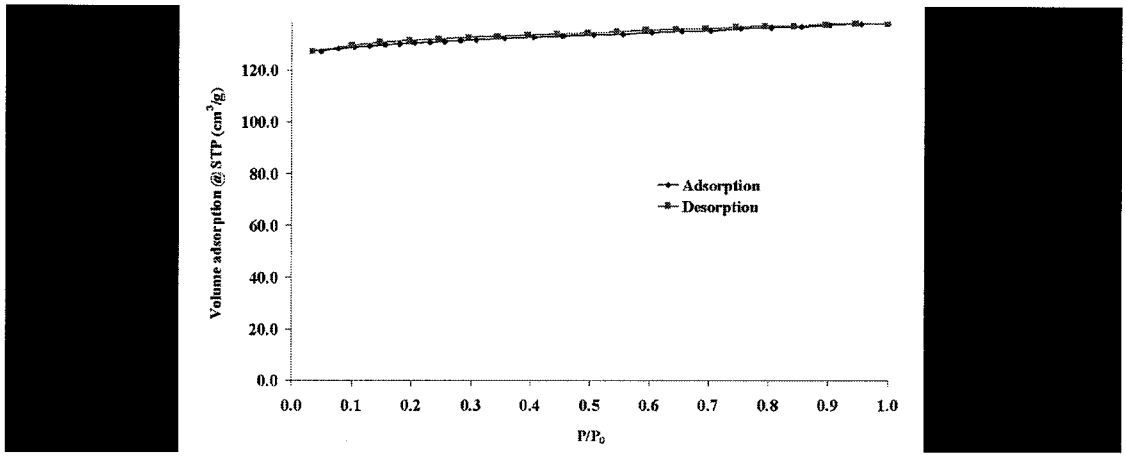

Figure 4. N_2 adsorption-desorption isotherm at 77 K on the synthesized NaK-LSX

internal pores are not restricted by a large cation. Moreover, the effect of a cation on the surface area and pore structure show that the ion-exchange processes could induce enormous changes in surface and pore structure and these ions inhibited the movement of nitrogen molecule into pores or the so-called pore blocking effect, resulting in the decrease in surface area (Langmi *et al.*, 2003; Rakoczy and Traa, 2003; Huang *et al.*, 2004).

Figure 5 shows cumulative pore volume and pore size distributions of NaK-LSX from N_2 adsorption. The pore diameter of NaK-LSX, shown in Figure 5(a), was calculated by the HK method and showed a narrow pore width between 0.3 - 1.9 nm with pore volume of 0.195 - 0.201 cm^3/g. Nevertheless, the curves of pore size distribution evaluated from desorption data by utilizing the BJH model shown in Figure 5(b) exhibited a narrow pore size distribution ranging from 1.3 - 30.0 nm with the highest pore size at 1.7 nm. However, a shoulder peak distribution is dominant and it was probably from interconnected surface pores of LSX (Chang *et al.*, 2005 and Lee *et al.*, 2006).

Table 3 shows results from a nitrogen adsorption study including the BET surface areas, pore volumes, and average pore diameters of NaK-LSX. The BET surface area and pore volume of NaK-LSX form RHS was interesting

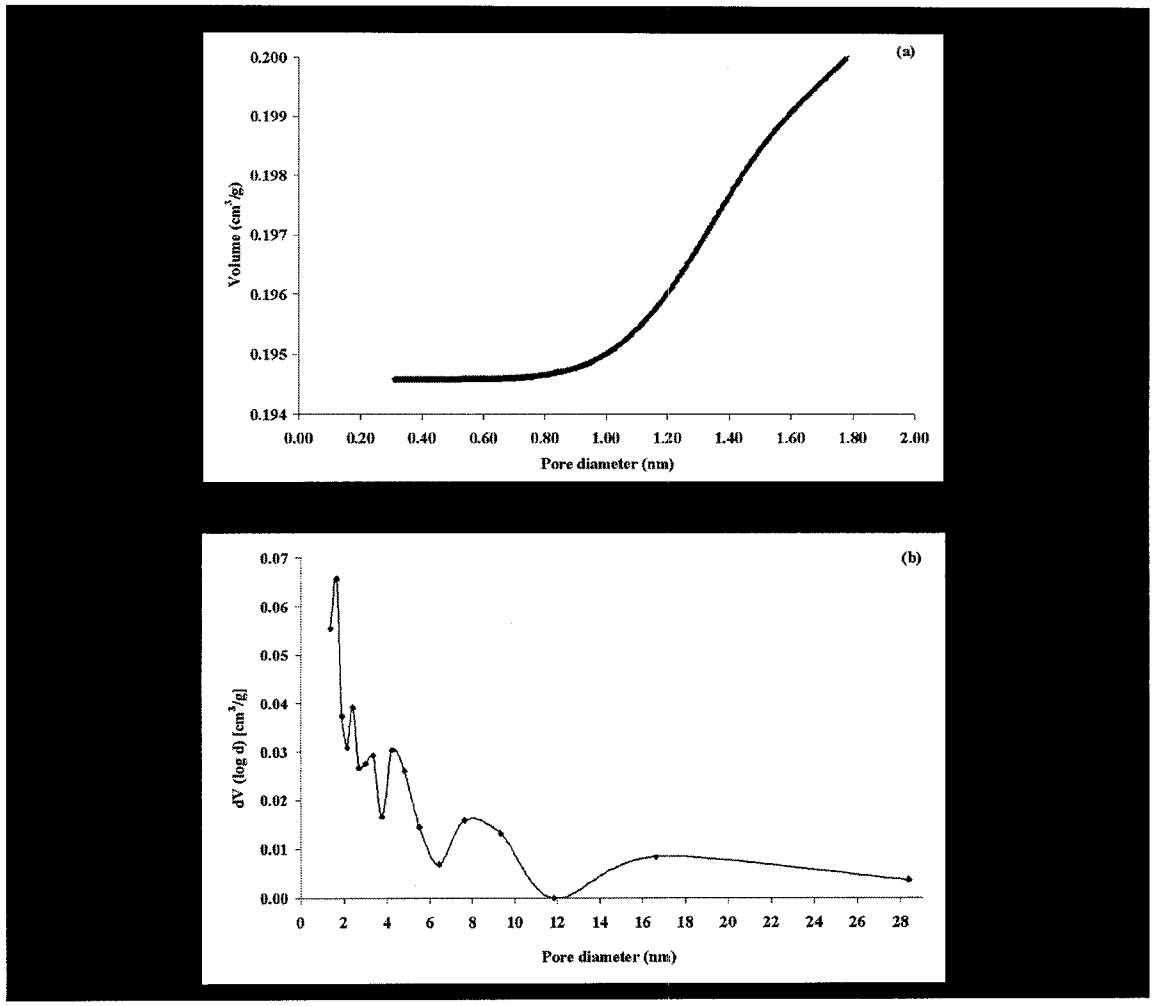

Figure 5. (a) HK cumulative pore volume and (b) BJH pore size distribution of NaK-LSX zeolite, where V is the cumulative pore volume (cm^3/g)

as it supported material for catalysis preparation or other application. (Langmi *et al.*, 2005)

Morphology of NaK-LSX Studied by SEM

Shape and size of NaK-LSX particles synthesized from RHS were studied by SEM and images are displayed in Figure 6 with magnification of 1,500 (a) and 25,000 (b). In the image with the smaller magnification, the solid product contained a mixture of multi-faceted spherulite crystals with a particle diameter approximately 6 - 10 mm along with round amorphous particles with a particle diameter approximately 0.2 - 5.0 mm. The multi-faceted spherulite particles were composed of polycrystal particles with different sizes along with small particles. Because some particles apparently connected with other particles, (Figure 5(a)), the particle size distribution was expected to be large as it was confirmed by DPSA (see next section). The particles in Figure 6(a) were distributed in the range of 0.3 - 10 μm with the largest contribution in the 0.3 - 2.0 μm range.

Particle Size Distribution of NaK-LSX by DPSA

The particle size distribution of Na-LSX was also investigated with DPSA and the results are presented as a histogram in Figure 7. The sizes were classified as oversize (area a) and undersize (area b), and the histogram plot

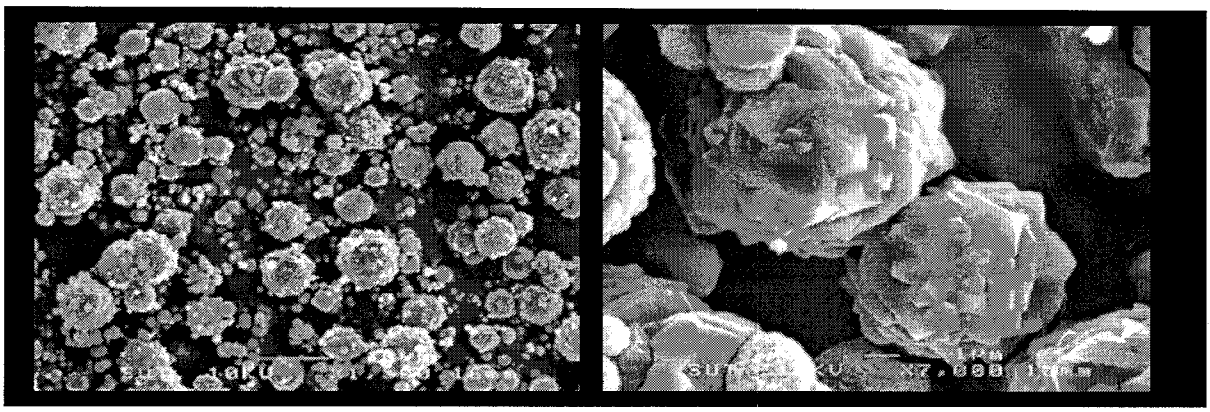

(a) (b)

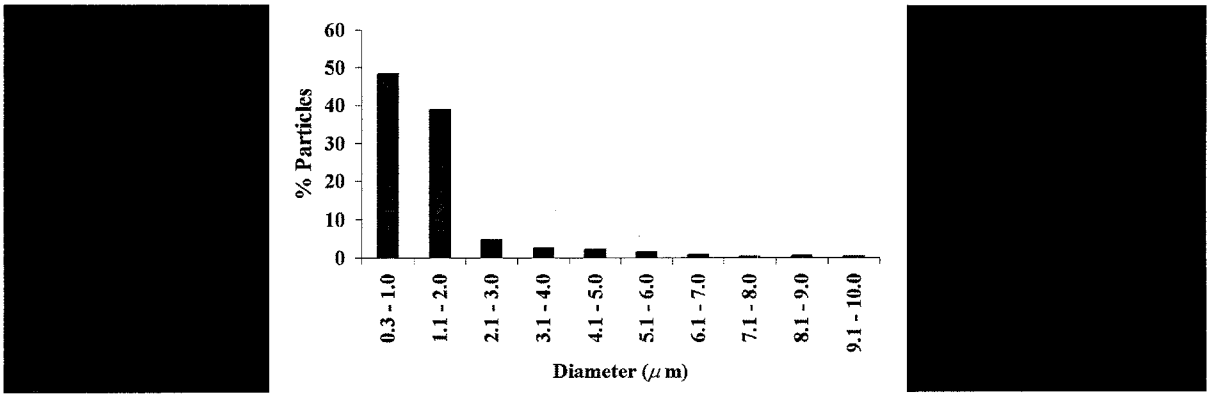

(c)

Figure 6. SEM images of synthesized Na-LSX with magnification of (a) 1,500 and (b) 25,000, respectively, and (c) particle size distribution measured from all particles in (a)

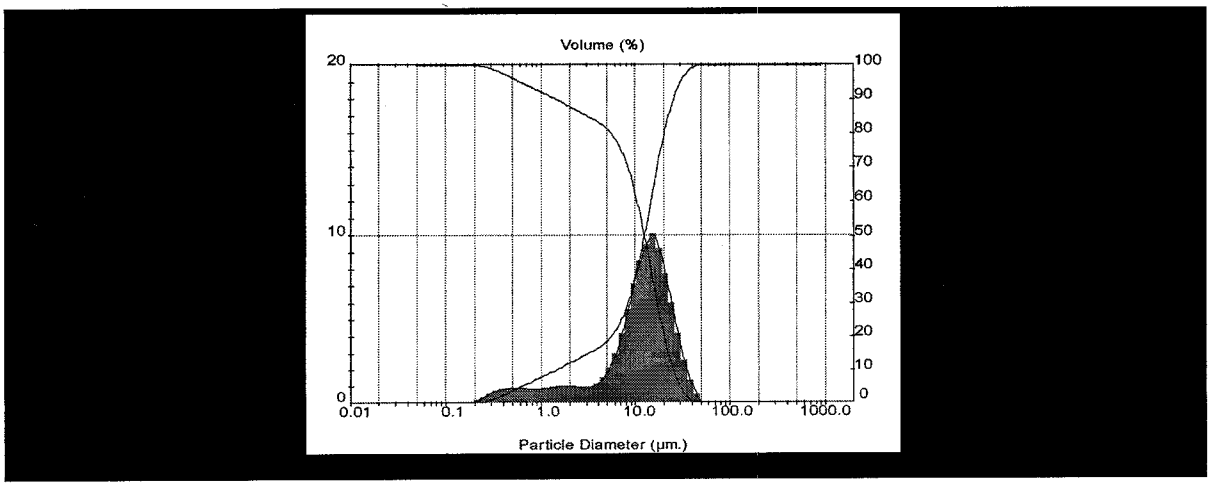

Figure 7. Particle size distribution of NaK-LSX synthesized from RHS; (a) percentage of sample below a certain size of particle, (b) percentage of sample above a certain size of particle and (c) histogram plot and frequency curve of particle

and frequency curves are (c). The histogram plot shows the percentage of volume of particles, and the height of the histogram bars (left hand scale) was at 15.0 - 17.5 μm as for the majority of particles. The peak frequency curve provided the apparent tail in particle size analysis and shows the dominantly single modal distributions at 5 - 50 μm. Note that the results from DPSA were the size and distribution of bulk particles which might be composed of several small particles clustered together, and thus were different from the results from SEM which displayed images of isolate particles. Because the shape of samples as seen in SEM varied from a spherical shape to multi-faceted spherulite, that caused a different light scattering or diffraction effect based on the angularity of the crystals and their hydrodynamic behavior suspension (Cundy and Cox, 2005).

Only the important part of the DPSA data was summarized in Table 4 because there were too many numbers in the full data. The particle size distribution of NaK-LSX at volume percentiles of 10 was above 1.43 μm, while that of 50 was 12.35 μm and that of 90 was below 24 μm. The large particle size distribution of zeolite X was common as Lee *et al.* (2006) reported that uniformly sized NaX was difficult to synthesize in a large single phase crystal because crystal nuclei grew rapidly during the crystallization period and might transfer into zeolite NaP which was a more stable phase.

Characterization and Thermal Stability of NH_4-LSX from Ion Exchange of NaK-LSX

LSX in ammonium form (NH_4-LSX) was prepared by ion exchange of NaK-LSX with a NH_4NO_3 solution and characterized by powder XRD. As shown in Figure 8(b), the resulting material still had all peaks positioned similarly to that of the standard NaX. The sequence of intensities was different from the standard NaX because of the difference in cation type as discussed earlier. The NH_4-LSX was also studied by SEM and the micrograph is displayed in Figure 9. Compared with the NaK-LSX in Figure 6(a), the exchanged zeolite contained more crystalline particles and the amorphous

Table 3. Textural properties of synthesized NaK-LSX zeolite

Textual Properties	Value	Unit
BET surface area[a]	391.4	(m^2/g)
External surface area[b]	361.0	(m^2/g)
Micro pore surface area[b]	355.3	(m^2/g)
Langmuir surface area[c]	577.1	(m^2/g)
Pore volume of micro pore[d]	0.19	(cm^3/g)
Micro pore diameter[e]	13.58	(nm)

[a]Multipoint BET analysis, [b]BJH analysis (t-method), [d]t-method, [e]DA method

Table 4. Percentile of NaK-LSX particle size distribution analyzed by DPSA

Statistic distribution of particle	Result (% volume)	Unit
d(0.1)	1.43	(μm)
d(0.5)	12.35	(μm)
d(0.9)	25.05	(μm)
Average diameter	13.23	(μm)
Span (width of distribution)	1.91	(μm)

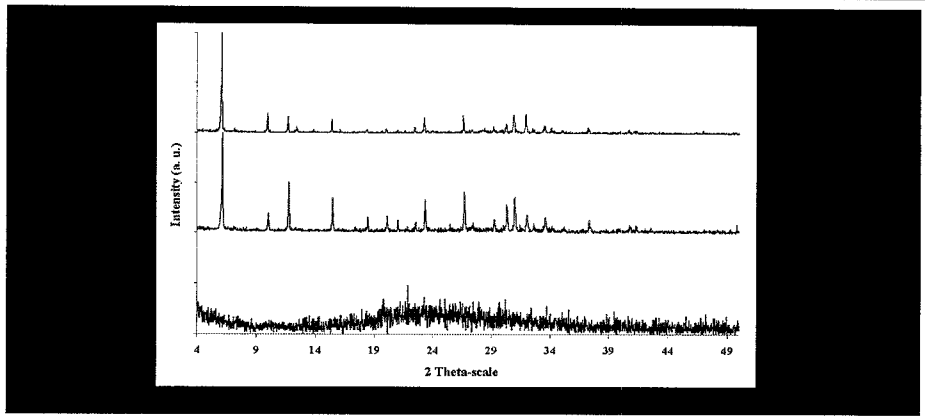

Figure 8. XRD patterns of (a) Na-LSX (b) NH_4-LSX, and (c) NH_4-LSX after calcination

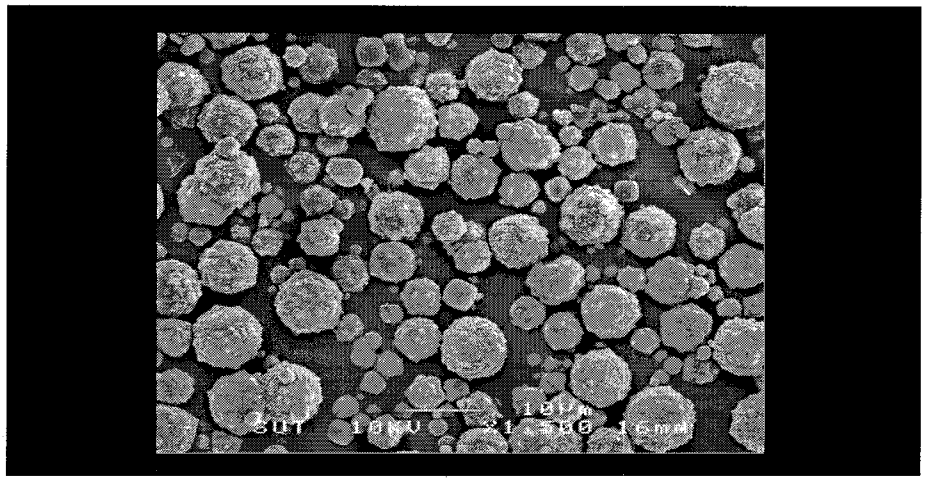

Figure 9. SEM images of NH_4-LSX with magnification of 1,500

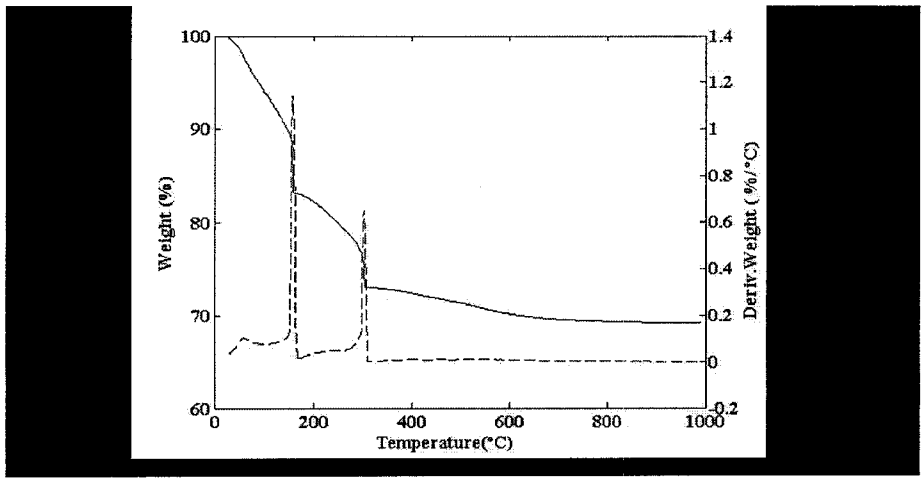

Figure 10. Thermogram of zeolite NH_4LSX (solid line is weight and dash line is first derivative of weight with respect to temperature)

particles might be removed with a basic solution during the exchange and wash process.

In general, zeolite in proton form can be obtained by calcination of ammonium form which releases ammonia. Thus, NH_4-LSX was calcined at 400°C for 3 h and the resulting material was characterized by XRD. As shown in Figure 8 (spectrum c), the characteristic peaks of zeolite X were no longer observed indicating the collapse of the NH_4-LSX structure to an amorphous form upon calcination. From this result, we investigated the thermal stability of NH_4-LSX by thermal analysis.

The thermal stability of NH_4-LSX was studied by thermal analysis. The results in Figure 10 demonstrated weight loss of NH_4-LSX when the temperature was raised from room temperature to 1,000°C, along with the first derivative of weight loss. When NH_4LSX was heated, there were three ranges of weight loss. The first range, with approximately 17% weight loss below 200°C, was attributed to removal of adsorbed water (Chandrasekhar and Pramada, 2001; Joshi *et al.*, 2002; Huang *et al.*, 2004). The second region with approximately 10% weight loss between 200°C and 300°C, was caused by the decomposition of NH_4^+ ion to ammonia and proton (Chandrasekhar and Pramada, 2001). The last region was a relatively small loss compared with the other two regions from 300°C to 650°C, possibly caused by loss of the structural hydroxyl group. No further weight loss was observed at a higher temperature. In general at the temperature range of 900 - 1,018°C, zeolite will be converted to mullite and glass phases (Chandrasekhar and Pramada, 2001; Esposito *et al.*, 2004).

Conclusions

RHS in amorphous phase with 98% purity was prepared by leaching rice husk with HCl acid and calcination, and used as a silica source for the synthesis of zeolite NaK-LSX. The formation of the zeolite structure was confirmed by XRD and FTIR. The NaK-LSX crystal morphology was multi-faceted spherulite particles as shown by SEM micrographs. The particle size distribution from DPSA shows a large scale in crystal size and size distribution. The BET surface area of the NaK-LSX was approximately 400 m^2/g. The ion-exchange with ammonium ions gives NH_4-LSX and the zeolite structure was still maintained after ion exchange. However, the structure collapsed after calcination to convert to proton form.

Acknowledgement

Funding for this research was from Suranaree University of Technology, the Thailand Research Fund (Contract number MRG4780147) and the National Synchrotron Research Center Research Fund (Grant 2-2548/PS01).

References

Auerbach, S.M., Carrado, K.A., and Dutta, K.P. (2003). Handbook of Zeolite Science and Technology. 1st ed. Marcel Dekker Inc., NY, 1p.

Chang, F.W., Kuo, W.Y., and Yang H.C. (2005). Preparation of Cr_2O_3-promoted copper catalysts on rice husk ash by incipient wetness impregnation. Appl. Catal. A-Gen., 288:53-61.

Chandrasekhar, S. and Pramada, P.N. (2001). Sintering behavior of ammonium exchanged low silica zeolites synthesized by two different routes. Ceram. Int., 27:351-361.

Chandrasekhar, S. and Pramada, P.N. (2002). Thermal study of low silica zeolites and their magnesium exchanged forms. Ceram. Int., 28:177-186.

Corma A. (2001). Zeolites as catalysts. In: Fine Chemicals Through Heterogeneous Catalysis. Sheldon, R.A. and Bekkum, H. (eds). Wiley-VCH, Weinheim, 80p.

Cundy, C.S. and Cox, P.A. (2005). The hydro-thermal synthesis of zeolites: Precursors, intermediates and reaction mechanism. Micropor. Mesopor. Mat., 82(1-2):1-78.

Dyer, A., Tangkawanit, S., and Rangsriwata-nanon, K. (2004). Exchange diffusion of Cu^{2+}, Ni^{2+}, Pb^{2+}, and Zn^{2+} into analcime

synthesized from perlite. Micropor. Mesopor. Mat., 75:273-279.

Esposito, S., Ferone, C., Pansini, M., Bonaccorsi, L., and Proverbio, E. (2004). A comparative study of the thermal transformations of Ba-exchanged zeolites A, X and LSX. J. Eur. Ceram. Soc., 24:2,689-2,697.

Grisdanurak, N, Chiarakorn, S., and Wittayakun, J. (2003). Utilization of mesoporous molecular sieves synthesized from natural source rice husk silica to chlorinated volatile organic compounds (CVOCs) adsorption. Korean J. Chem. Eng., 20:950-955.

Huang, F.-C., Lee, J.-F., Lee, C.-K., and Chao, H.-P. (2004). Effects of cation exchange on the pore and surface structure and adsorption characteristics of montmorillonite. Colliod. Surface. A, 239:41-47.

Huang, S., Jing, S., Wang, J., Wang, Z., and Jin, Y. (2001). White silica obtained from rice husk in fluidized propellant bed. Powder Technol., 117:232-238.

Joshi, U.D., Joshi, P.N., Tamhankar, S.S., Joshi, V.P., Idagec, B.B., Joshid, V.V., and Shiralkar, P.V. (2002). Influence of the size of extraframework monovalent cations in X-type zeolite on their thermal behavior. Thermochim. Acta, 387:121-130.

Kapur, P.C. (1985). Production of reactive bio-silica from the combustion of rice husk in a tube-in-basket (TiB) burner. Powder Technol., 44:63-67.

Katsuki, H., Furuta, S., Watari, T., and Komarneni, S. (2005). ZSM-5 zeolites/porous carbon composite: Conventional-and microwave-hydrothermal synthesis from carbonized rice husk. Micropor. Mesopor. Mat., 86:145-151.

Khemthong, P. and Wittayakun, J., (2006). Synthesis and characterization of Zeolites Y from rice husk silica. Proceedings of the 32nd Congress on Science and Technology of Thailand; October 10 - 12, 2006; Thailand, 163p.

Kühl, G. (2001). Low silica type X. In: Verified Syntheses of Zeolitic Materials. 2nd ed. Robson, H. (ed). Elsevier Science B.V., Amterdam, p. 153-154.

Langmi, H.W., Walton, A., Al-Mamouri, M.M., Johnson, S.R., Book, D., Speight, J.D., Edwards, P.P., Gameson, I., Anderson, P.A., and Harris, I.R. (2003). Hydrogen adsorption in zeolites A, X, Y and RHO. J. Alloy. Compd., 356-357:710-715.

Langmi, H.W., Book, D., Walton, A., Johnson, S.R., Al-Mamouri, M.M., Speight, J.D., Edwards, P.P., Harris, I.R., and Anderson, P.A. (2005). Hydrogen storage in ion-exchanged zeolites. J. Alloy. Compd., 404-406:637-342.

Lee, H.J., Kim, Y.M., Kweon, O.S., and Kim, I.J. (2006). Structural and morphological transformation of NaX zeolite crystals at high temperature. J. Eur. Ceram. Soc., 27(2-3):561-564.

Li, Y. and Yang, T.R. (2006). Hydrogen storage in low silica type X zeolites. J. Phys. Chem. B., 110:17,175-17,181.

Liou, T.H. (2004). Preparation and Characterization of nano-strucutred silica from rice husk. Mat. Sci. Eng. A, 364:313-323.

Park, B.D. (2003). Characterization of anatomical features and silica distribution in rice husk using microscopic and micro-analytical techniques. Biomass and Bioenerg., 25:319-327.

Prasetyoko, D., Ramli, Z., Endud, S., Hamdan, H., and Sulikowski, B. (2006). Conversion of rice husk ash to zeolite beta. Waste Manage., 26:1,173-1,179.

Rakoczy, R.A. and Traa, Y. (2003). Nanocrystalline zeolite A: synthesis, ion exchange and dealumination. Micropor. Mesopor. Mat., 60:69-78.

Roberie, T.G., Hildebrandt, D., Creighton, J., and Gilson, J.-P. (2001). Preparation of zeolite catalysts. In: Zeolites for Cleaner Technologies. Guisnet, M. and Golson, J.-P. (eds). Catalytic Science Series. Imperial College Press, London. (3):57-63.

Sang, S., Liu, Z., Tian, P., Liu, Z., Qu, L., and Zhang, Y. (2006). Synthesis of small crystals zeolite NaY. Mater. Lett., 60:1,131-1,133.

Sun, L. and Gong, K. (2001). Silicon-based

material from rice husks and their applications. Ind. Eng. Chem. Res., 40:5,861-5,877.

Tangkawanit, S. and Rangsriwatananon, K. (2004). Synthesis and kinetic study of zeolite from Lopburi perlite. Suranaree J. Sci. Technol., 12(1):61-68.

Wang, H., Lin, P.K.S., Huang, Y.J., Li, M.C., and Tsaur, L.K. (1998). Synthesis of zeolite ZSM-48 from rice husk ash. J. Hazard. Mater., 58:147-152.

Williams, P.T. and Nugranad N. (2000). Comparison of products from the pyrolysis and catalytic pyrolysis of rice husks. Energy, 25:493-513.